

Investigation of the Orthogonal Blade-Vortex Interaction

2nd Interim Report

by

J.M. Early* & R.B. Green†

Department of Aerospace Engineering
University of Glasgow
Glasgow
G12 8QQ
Scotland

prepared for

USARDG-UK
Edison House
223 Old Marylebone Road
LONDON
NW1 5TH
United Kingdom

under

contract N68171-00-M-5988

R&D 89104-AN-01

Contract period 1st December 2000 to 28th February 2001

22nd February 2001

* Research student
† Principal Investigator

REPORT DOCUMENTATION PAGE

Form Approved
OMB No. 0704-0188

Public reporting burden for this collection of information is estimated to average 1 hour per response, including the time for reviewing instructions, searching existing data sources, gathering and maintaining the data needed, and completing and reviewing this collection of information. Send comments regarding this burden estimate or any other aspect of this collection of information, including suggestions for reducing this burden to Washington Headquarters Services, Directorate for Information Operations and Reports, 1215 Jefferson Davis Highway, Suite 1204, Arlington, VA 22202-4302, and to the Office of Management and Budget, Paperwork Reduction Project (0704-0188), Washington, DC 20503.

1. AGENCY USE ONLY (Leave blank)	2. REPORT DATE	3. REPORT TYPE AND DATES COVERED
	22nd February 2001	Interim. 1st Dec. 2000 to 28th Feb. 2001
4. TITLE AND SUBTITLE		5. FUNDING NUMBERS
Investigation of the Orthogonal Blade-Vortex Interaction 1st Interim Report		N68171-00-M-5988
6. AUTHOR(S) J.M. Early, R.B. Green		
7. PERFORMING ORGANIZATION NAME(S) AND ADDRESS(ES) Department of Aerospace Engineering University of Glasgow Glasgow Scotland G12 8QQ		8. PERFORMING ORGANIZATION REPORT NUMBER G.U. Aero report number 0103
9. SPONSORING / MONITORING AGENCY NAME(S) AND ADDRESS(ES) USARDSG-UK Edison House 223 Old Marylebone Road LONDON NW1 5TH UK		10. SPONSORING / MONITORING AGENCY REPORT NUMBER

11. SUPPLEMENTARY NOTES

12a. DISTRIBUTION / AVAILABILITY STATEMENT Approved for public release Distribution is unlimited	12b. DISTRIBUTION CODE
--	------------------------

13. ABSTRACT (Maximum 200 Words)

Preliminary results from a PIV study of the orthogonal blade-vortex interaction are presented. This report presents a comparison of the details of the orthogonal BVI over the lower and upper surfaces of the blade. Detailed differences in the mechanics of these interactions have been noted. Features of the vortex behaviour in the wake of the blade are also presented together with the results obtained at very close proximity to the blade surface.

14. SUBJECT TERMS Blade-vortex interaction, PIV, unsteady aerodynamics, vortex flows, helicopters, aerodynamic testing		15. NUMBER OF PAGES 5+12	
		16. PRICE CODE	
17. SECURITY CLASSIFICATION OF REPORT Unclassified	18. SECURITY CLASSIFICATION OF THIS PAGE Unclassified	19. SECURITY CLASSIFICATION OF ABSTRACT Unclassified	20. LIMITATION OF ABSTRACT UL

NSN 7540-01-280-5500

Standard Form 298 (Rev. 2-89)
Prescribed by ANSI Std. Z39-18
298-102

Investigation of the Orthogonal Blade-Vortex Interaction

2nd Interim Report

by

J.M. Early^{*} & R.B. Green[†]

Department of Aerospace Engineering
University of Glasgow
Glasgow
G12 8QQ
Scotland

prepared for

USARDSG-UK
Edison House
223 Old Marylebone Road
LONDON
NW1 5TH
United Kingdom

under

contract N68171-00-M-5988

Contract period 1st December 2000 to 28th February 2001

22nd February 2001

^{*} Research student

[†] Principal Investigator

Abstract

This report presents a comparison of the details of the orthogonal BVI over the lower and upper surfaces of the blade. Detailed differences in the mechanics of these interactions have been noted. Features of the vortex behaviour in the wake of the blade are also presented together with the results obtained at very close proximity to the blade surface.

1 Experimental Investigation of the Orthogonal BVI

The images for the orthogonal interaction are presented with the axis relative to the leading edge position, unless otherwise stated.

1.1 Isolated Vortex Measurements

In order to obtain a comparative set of results for the orthogonal interaction, measurements of the vortex within the freestream have been obtained. As previously documented in investigations utilising this experimental rig (Green et al, 1999, Doolan et al, 2000), it may be confirmed that in the freestream state, the vortex has a core diameter of 15mm, with a mean circulation strength of approximately $0.58\text{m}^2\text{s}^{-1}$ (figure 1(a) and (b)).

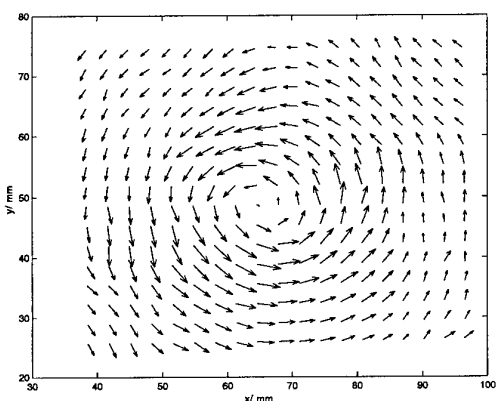


Figure 1(a) Mean u component removed
Maximum Velocity
Axis is Arbitrary

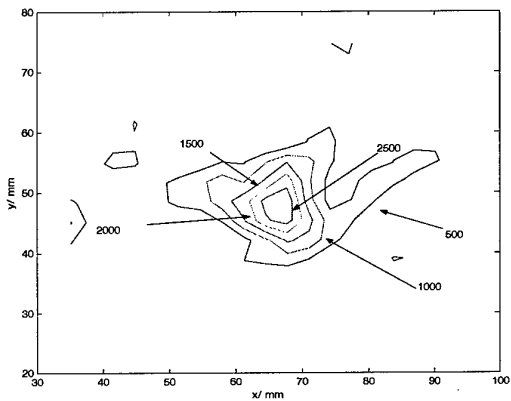


Figure 1(b) Vorticity contours

Data from the isolated vortex will assist in isolating the interaction effects.

1.2 Progression of the Interacting Vortex over the Lower and Upper Surfaces

By utilising the dual PIV system, it has been possible to track a single interacting vortex on either side of the blade surface, and make direct comparison of the effect on each part of the severed vortex. As the vortex passes over the lower surface, a spiralling motion outward of the vortex core, as previously noted (Early and Green, 2000), is observed, with this effect usefully represented by a point source superimposed onto a potential vortex. This spiralling motion leads to a decrease in the peak vorticity levels associated with the vortex as it progresses over the blade as vorticity is redistributed radially outwards. The corresponding case for the cut vortex passing over the upper surface location shows a significant difference, with an inward spiralling evident in the core, again noted previously. This may again be compared to a point sink placed onto the potential vortex, but in this case the sink component is of a much lesser strength than the source flow on the lower surface. As the vortex progresses over the upper surface, there does not appear to be any real disturbance to the peak vorticity levels, indicating that there is little re-distribution of vorticity within the core. It is useful to note that the upper surface interaction is not simply an inverted lower surface interaction

Variation in the core area on the lower surface has already been tracked in order to highlight the core bulging on the lower surface with increasing distance from the blade surface, and corresponding analysis of the core radius on the upper surface has been carried out. Variation in the upper surface core is less evident than on the lower surface, with a very gradual increase in the core area as it moved further away from the blade

As previously discussed (Early and Green, 2000), it is possible to infer certain characteristics of the vortex axial flow through consideration of the divergence within the flowfield. Analysis of the divergence pattern can provide an indication of the strength of the interaction. On the lower surface (figure 2(a)), the divergence contours indicate that the axial flow is decelerating towards the blade, as would be expected. With progression over the blade surface, the core may be observed to continue to expand as a result of the effect on the axial flow of the interaction. Analysis of the

divergence on the upper surface (figure 2(b)), however, reveals that the effect on the vortex core is not as simple. The core region is surrounded by areas of both positive and negative divergence, which persist over the chord of the blade. This type of pattern may be resolved by considering the necessary mass flow requirements. The area of negative divergence would be indicative of the axial flow decelerating close to the blade surface, as would be expected, but the positive area a requirement in order to re-establish the axial flow further away from the blade surface. The presence of this pattern has been examined for possible error, with the use of post-processing steps, tile overlapping and variation of tile size, all of which have confirmed that this pattern is not a response to spurious vectors.

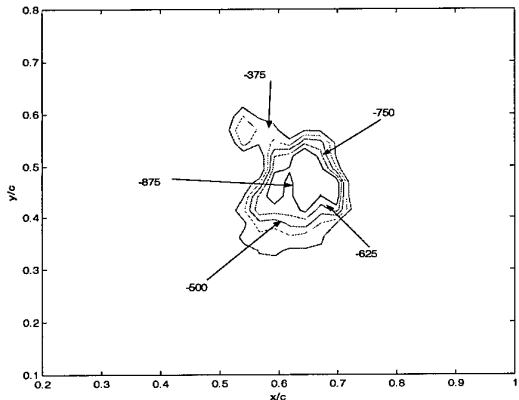


Figure 2(a) Lower Surface

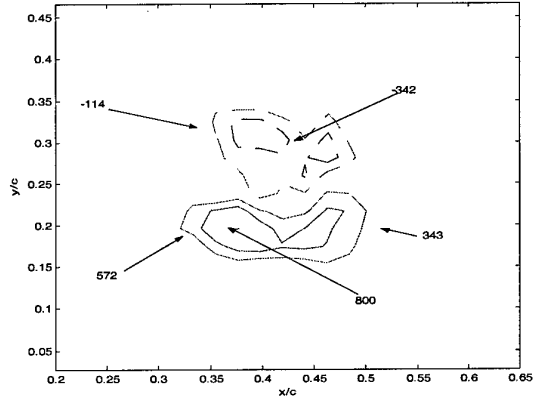


Figure 2(b) Upper Surface

Figure 2 Comparison of Lower and Upper Surface Divergence Contours (Lightsheet positioned 15mm from blade centreline for each interaction case)

1.3 Interaction behind the Trailing Edge

For interrogation of the trailing edge region, the lightsheet was placed coincident with the chordline of the blade behind the trailing edge. The position of the lightsheet relative to the blade was then altered laterally in order to attain comparative data for the upper and lower surface locations.

Passing into the trailing edge region, a definite decrease in the peak vorticity when compared with the pre-interaction case was immediately evident just behind the blade. This is also held for the upper and lower surface regions. Probably most surprising in this area was the level of coherence still evident in the structure of the vortex, with no major distortion within the core due to the wake of the blade apparent (figures 3(a) and (b)). Behind the blade on either side behind the blade there was no evidence of a radial flow within the core.

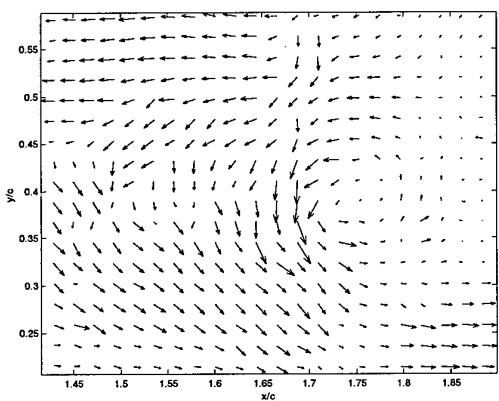


Figure 3(a) Trailing Edge Location Maximum Velocity 7.34ms^{-1}

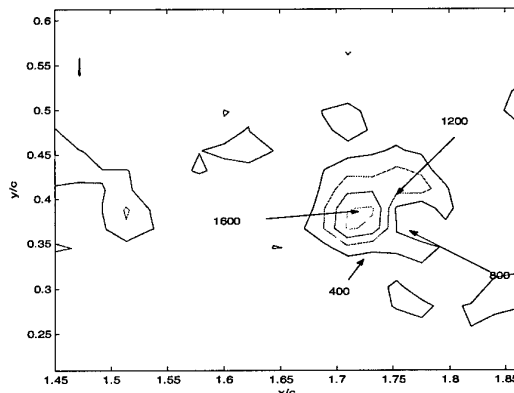


Figure 3(b) Vorticity contours

Previous work looking at the interaction of a pre-cut vortex (Doolan et al, 2000) has suggested that axial and tangential components of the vortex are re-established after passing over the trailing edge. The current investigation concurs with the re-establishment of the tangential components, and although the measurements taken would not allow any conclusions to be made about the nature of the axial flow, the flow in the out-of-plane direction does not appear to be undergoing any acceleration. This would indicate the possibility that the re-joining of the two halves of the vortex core

may occur, but would require further investigation in order to confirm this. In order to fully examine the possible reformation of the vortex, the flow behind the trailing edge will be examined from a downstream location, so the axial flow component may be observed.

1.4 Boundary Layer Investigation

In order to examine the development of the interaction very close to the blade surface, an alternative experimental setup was necessary. A 360mm long, 6mm thick glass plate was mounted in the working section of the wind tunnel. Visualisation of the interaction of the vortex close to the boundary layer was therefore possible with the lightsheet 2mm from the plate surface. Measurements for both lower and upper surface representations have been attained. Initial analysis of the lower surface has revealed a significant distortion within the core, which has led to the vortex appearing to be relatively disorganised in structure (figures 4(a) and (b)). The disorganised pattern is not reflected in the divergence contours (not shown) which still indicate a deceleration of the flow towards the plate, and therefore that the interaction is continuing.

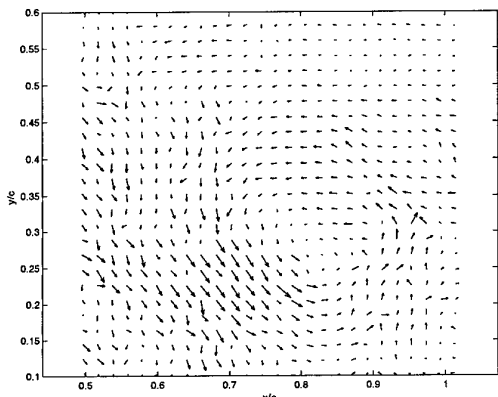


Figure 4 (a) Lower Surface Boundary Layer Mean u component removed

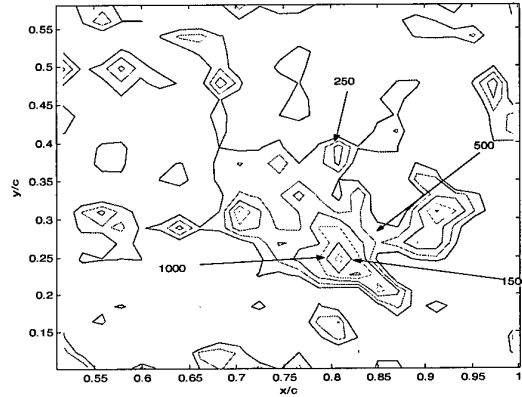


Figure 4 (b) Vorticity contours

Due to the nature of this distortion, it is most likely to be attributed to the impingement of the axial flow onto the surface of the plate, and the proximity at which this is occurring.

The upper surface interaction, is however, not promoting the same level of distortion, and a clear vortex is still evident. Peak vorticity levels at this level appear to be extremely high (figures 5(a) and(b)).

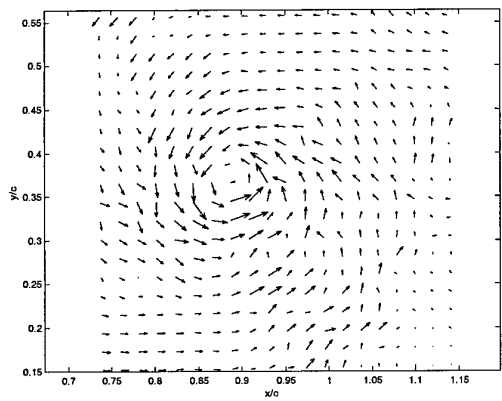


Figure 5 (a) Upper Surface Boundary Layer

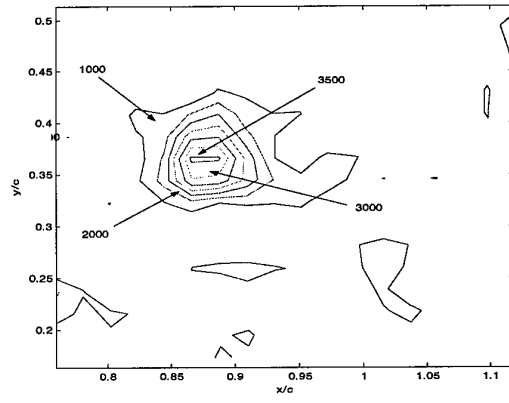


Figure 5 (b) Vorticity Contours

Following on from the work done on the blade upper surface, the divergence patterns from the boundary layer interaction still indicates that the vortex core consists of areas of both positive and negative divergence, as observed further away from the blade surface.

1.5 Conferences and Publications

The conference paper for the Royal Aeronautical Society Aerodynamics Research Conference has been completed and submitted, and is to be presented at the conference on the 10th April 2001. (See Appendix). An abstract for the 4th International Symposium on Particle Image Velocimetry in Göttingen, Germany (September 2001) is to be submitted.

2. Research plans for remainder of contract period

The current priority is to complete the experimental programme. No further rig development is necessary, and the only significant obstacle to completing the test programme is available tunnel time. It is anticipated that the test programme will be completed in the next quarter. At other times the focus will be upon data analysis so that a clear picture of the physical nature of the orthogonal BVI may be built up. It is anticipated to visit the USA to report findings in the final quarter of the research period; late July would be the most convenient time for this.

3. Administrative actions

3.1 Staffing

No changes in the staffing have been necessary. Ms. Early has continued on the project as the research assistant.

3.2 Conference submission

An abstract was submitted for a presentation at the 4th International PIV workshop in Gottingen, Germany. This meeting takes place in September 2001.

A paper was prepared for the Royal Aeronautical Society Aerodynamics conference on 9th & 10th April 2001. This meeting is attended by most UK universities with research interests in aerodynamics.

4. References

Green & Doolan (1999) "PIV Measurements of the Orthogonal Blade-Vortex Interaction" 3rd International Workshop on PIV, Santa Barbara

Doolan et al (2000) "Surface Pressure Measurements of the Orthogonal Blade-Vortex Interaction" accepted for publication AIAA Journal

Early & Green (2000) "Investigation of the Orthogonal Blade-Vortex Interaction" G.U. Aero Report 0012

Appendices

A. Financial statement

A breakdown of the funds so far used is as follows (exchange rate 22nd February 2001 £1 = \$1.443) :

Equipment	£0	
Studentship	£2566	\$3703
Consumables	£1532	\$2211
Technician salary	£373	\$538
Total	£4471	\$6452
Balance remaining	£10875	\$15693

B. Important property acquired during present report period

Significant consumables included essential optics for beam delivery, a repair to a laser and a spares for maintenance on the rotor rig.

C. RaeS Conference Report

FLOW VISUALISATION OF THE ORTHOGONAL BLADE-VORTEX INTERACTION USING PARTICLE IMAGE VELOCIMETRY

J.M. Early, R.B. Green, F.N. Coton
Department of Aerospace Engineering
University of Glasgow
Glasgow
G12 8QQ

Abstract

The flow field produced by the Orthogonal Blade Vortex Interaction (BVI) was examined through the application of a particle image velocimetry (PIV) technique, and acquisition of comparative unsteady surface pressure measurements.

At the leading edge, a pressure peak occurred where the core flow was directed towards the blade (lower surface), and a corresponding suction peak occurred on the opposing side (upper surface). The equivalent velocity vector maps revealed that a significant radial flow from the vortex core exists after the core was severed, in the form of an outward flow from the core centre on the lower surface, and inward on the upper. With the progression of the vortex over the chord of the blade, the interaction led to a decrease in peak vorticity on the lower surface, but a steady level was maintained on the upper surface. Calculation of the divergence of the flow field has allowed an assessment of the effect of the interaction on the axial flow acceleration, and has revealed that after the initial cut, there is no further variations in the axial flow on either side of the blade.

A simple model of the flow in the form of a source/sink and vortex was developed, which is illustrative of the physical features of the BVI.

Surface pressure measurements in the trailing edge region indicate that the two halves of the core rejoin, re-establishing both radial and axial components in a weakened form, and the velocity measurements agree with this supposition.

Nomenclature

- c interacting blade chord, (m)
 C_M $\frac{1}{4}$ pitching moment coefficient,
[$M/(1/2 \rho V_\infty^2 c^2)$]
 C_N normal force coefficient, [$N/(1/2 \rho V_\infty^2 c)$]
 C_p pressure coefficient, [$(p-p_\infty)/(1/2 \rho V_\infty^2)$]

M	$\frac{1}{4}$ chord pitching moment/unit span, (N)
N	normal force per unit span, (Nm^{-1})
q	source/sink strength, ($m^2 s^{-1}$)
t	time, (s)
u	streamwise velocity component, (ms^{-1})
v	normal velocity component, (ms^{-1})
w	cross stream velocity component, (ms^{-1})
V_∞	free stream velocity, (ms ⁻¹)
x	length streamwise, (m)
y	length normal, (m)
z	length cross stream, (m)
α	angle of incidence, (deg)
ϑ	angle, (deg)
Γ	circulation ($m^2 s^{-1}$)
ρ	freestream density, ($kg m^{-3}$)

1 Introduction

The strong trailing tip vortices that are shed from the main rotor blades dominate the wake of the main rotor of a helicopter. In forward flight, this wake may be observed to be skewed backwards by the oncoming flow. Since these vortices tend to be persistent, without fully dissipating for several rotor revolutions, an interaction between the trailing vortex and the tail rotor assembly occurs. The orthogonal blade-vortex interaction is one of the modes associated with this.

This type of interaction is just one of many that contributes to the acoustic and vibratory problems that are associated with rotorcraft operation. Much research has been carried out into the phenomena of BVI, with the tail rotor interaction becoming of interest in the last few years. Experimental and computational modelling¹⁻⁶ have both been employed in order to build up a clearer picture of this complex interaction. Initial mathematical modelling introduced the theory of the vortex 'shock' (Marshall, 1994)⁷, formed as a result of the impingement of the core axial flow onto the surface of the blade. A corresponding expansion wave is observed on the opposite side of the blade. These waves control the core bulging when the axial flow is directed towards the surface and thinning when it is directed away, and evidence of this has been

produced through water flow visualisation (Marshall & Krishnamoorthy, 1997)⁸, as well as showing the production of secondary vorticity and entrainment of the boundary layer fluid into the vortex core. Inviscid flow theory modelling (Lee et al, 1998)⁹ has shown that when the axial flow is directed towards the blade surface, the vorticity of the core is redistributed radially outwards, leading to a decrease in maximum vorticity levels. This type of radial outflow has also been visualised with PIV (Green et al., 2000)¹⁰, which has again been attributed to the impingement of the axial flow onto the blade surface.

Although there is much previous work on the blocking of the axial flow, less is known about the interaction where the flow is directed away from the blade surface. This paper describes the application of PIV to the orthogonal blade vortex interaction in order to track the progression of the vortex over both sides of the interacting blade from the leading edge position to the trailing region, and a series of surface pressure measurements for the same kind of interaction. The effect of incidence on this interaction is also considered.

2 Experimental Method

Experimental investigation of the Orthogonal Blade Vortex interaction has been carried out in the 1.15 x 0.85m closed return, low speed wind tunnel at the University of Glasgow. A vortex generator situated in the contraction produced three-dimensional vortices for simulation of the interaction in the working section. The design of this generator has been described in detail in many previous studies^{11,12}, and consists mainly of a rotor of radius 0.75m, with a single rectangular planform blade of NACA 0015 cross section and a chord of 0.1m. The variation of pitch during rotation is accomplished through the use of a spring loaded pitch link running on a cylindrical cam. The important feature of the vortex generator is that it produces vortices with a significant axial velocity component. This is essential for correctly modelling the orthogonal BVI. The tail rotor interaction is modelled by the collision of the three-dimensional convecting vortices with a symmetric, stationary blade, of NACA 0015 cross section and chord 152.4mm, spanning the wind tunnel working section. It is positioned 12 to 13 chordlengths downstream of the rotor centreline, and at an offset of 225mm from the wind tunnel centre line (figure 1 a and b). This offset has previously been identified¹³ as the location within the

working section where the vortex axis is approximately 90° to the mean flow, with minimal effect from the wake of the rotor shaft observed, which may obscure the blade.

Instrumentation of the blade allowed for surface pressures to be recorded during the interaction, allowing both transient normal force and quarter chord pitching moment data to be acquired, and the effect of the blade incidence relative to the oncoming flow to be examined.

Independent velocity measurements of the interaction were also obtained, by studying the interaction with an uninstrumented blade using a particle image velocimetry (PIV) system^{14,15} (see section 2.2).

For all testing, the wind tunnel speed was set to 20m/s, and the rotor rig to 520 rpm, giving a nominal blade Reynolds number of 2×10^5 . These parameters have previously been defined¹³ as the most suitable for the production of a useful vortex in the wind tunnel working section.

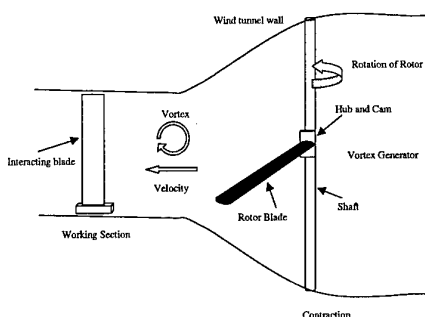


Figure 1a: Wind tunnel experimental setup

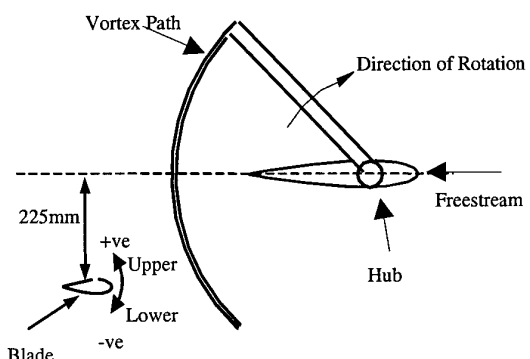


Figure 1b: Plan view of experimental setup

2.1 Acquisition of Pressure Data

The blade was instrumented at 78.5% span, with a chordal array of 30 miniature Kulite pressure transducers mounted around the surface of the blade. The transducers were connected to a surface orifice of 1mm diameter.

Pressure data for each transducer was recorded using a BE256 data logger in a single 32000 sample block at 20 kHz sampling rate. The sample rate and size allowed approximately 13 rotor revolutions of data capture. Five blocks of data were obtained at each blade incidence. The data logger and software employ automatic gain adjustment features, allowing measurements to obtain at the maximum resolution possible for the system. On the basis of previous measurements obtained using the Kulite miniature transducers, the uncertainty in any measured pressure coefficients is estimated to be 0.5%, and that of the force and pitching moment coefficient to be 2.1%.

2.2 PIV System

2.2.1 Acquisition of PIV data

The illumination for the PIV system is provided by two Spectra Physics GCR-13-10 frequency doubled, double pulsed Nd:YAG lasers, which run at a nominal repetition rate of 10Hz, with a pulse width of 8ns. The beams produced are passed into the wind tunnel working section through the use of a beam shaping telescope and a cylindrical lens arrangement. The lightsheets were arranged parallel to the blade chordline, a short distance away from the blade surface. Seeding is provided by a smoke generator, introducing Shell Ondina E.L. 'oil mist' into the flow, each particle having a nominal diameter of 2 μ m. The interaction is then photographed using two eight bit Kodak Megaplus ES 1.0 digital cameras, each of 1k x 1k resolution, operating in triggered double-exposure mode. The cameras are used in two positions for image capture, either on both sides of the wind tunnel working section to capture progression over the lower and upper surfaces, or on the same side of the tunnel to track the progression of the vortex over one side of the blade. Images have also been obtained using only a single camera arrangement.

Image capture was performed using two National Instruments PCI 1424 digital frame grabbers, with the synchronisation of the

cameras, frame grabbers and laser synchronisation system programmed and controlled through LabVIEW on a PC. The inter-pulse separation of each laser was 35 μ s. In single pulse mode, the laser has a maximum pulse energy of 150mJ, but with a 35 μ s delay in double pulse mode, this is significantly reduced.

2.2.2 Data Analysis

The analysis of the PIV images and vector validation were carried out simultaneously through the application of a standard FFT and a window shifting technique. The validation method is referred to as the Forward/Reverse Tile Test (FRTT)⁹. This technique involves splitting the image pairs into a series of discrete, equally sized adjacent tiles (typically 32x32 pixels), and calculation of the mean particle image displacement for each tile using a standard FFT and sub-pixel accurate detection routine. Two new tiles and their associated particle image displacements are then defined from this. From the comparison of the central vector with the two projected vectors, wild vectors may be significantly reduced within the flow field (as shown by Green et al, 2000). The calculated pixel displacements are then converted into equivalent spatial displacements using a transfer function, which represents a photograph of a calibration grid placed in the working section of the wind tunnel within the illuminated region. The grid is typically a 10cm x10cm regularly spaced array of dots, each at 5mm intervals. A local co-ordinate system based on the centroid of each of these dots may then be used to evaluate the local transfer functions. This accounts for stretching and rotation of the image due to the camera lens. The accuracy of the velocity vectors associated with this would be in the region of 2 – 4%.

Post processing steps may also be employed in order to further reduce the number of wild vectors appearing in the vector maps. The most common approach taken for this comprises of data validation and interpolation (as described by Noguiera et al, 1997)¹⁶. It should be noted that a high level of such vectors may be found within the vortex core, due to the ejection of the smoke particles by the relatively high rotational velocity gradient which exists within the vortex core.

In order to calculate the vorticity within the core, the vorticity for one tile was calculated by a circulation method. This is then averaged

over four adjacent tiles in order to reduce the effect of errors present within the flow.

2.2.3 Divergence Field Calculation

The dynamics of the orthogonal interaction have previously been identified to be governed by the impingement of the axial flow onto the surface of the blade. Understanding the effect of the interaction on the axial flow is therefore of importance. The PIV technique only allows for measurements to be taken in two-dimensional space. In order to obtain a three-dimensional view of the interaction, there are several possible options. Stereoscopic PIV is one option, which allows three-dimensional data to be obtained using two images of a single region with a known angular offset. Another method, and the one adopted for this study, is the extraction of three-dimensional data from a single two-dimensional image.

By considering the continuity equation for unsteady flow, a relationship between the particle displacements within the streamwise x and normal y planes may be built up with the cross-stream z component.

$$\frac{\partial \rho u}{\partial x} + \frac{\partial \rho v}{\partial y} + \frac{\partial \rho w}{\partial z} + \frac{\partial \rho}{\partial t} = 0 \quad (\text{I})$$

As the flow regime under inspection is subsonic, and as such may be treated as incompressible, this may be simplified to

$$\frac{\partial w}{\partial z} = - \left(\frac{\partial u}{\partial x} + \frac{\partial v}{\partial y} \right) \quad (\text{II})$$

Through the calculation of the divergence associated with the u and v components of velocity, detail of the flow behaviour in the third dimension made be made without the use of a stereoscopic system.

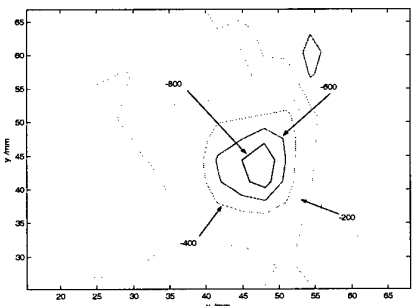


Figure 2: Typical divergence pattern for the lower surface interaction

The results obtained by this method are sensitive to any velocity errors, and in order to achieve an accurate representation, averaging over nine adjacent tiles is required.

3. Results and discussion

3.1 Pressure Data

The following pressure data has previously been presented by Doolan et al (2000)¹¹. It is repeated here for completeness within the current work.

3.1.1 Pressure variation at zero degrees incidence

For the basic orthogonal interaction at zero degrees incidence, the unsteady blade pressures were converted into pressure coefficients using the recorded freestream velocity, air density and pressure. The temporal variation of the recorded pressure as the vortex is cut is shown, with the steady component of the pressure signal removed for clarity. This steady component is determined through the averaging of 32000 pressure samples obtained while the generator was idle.

For the presented results, $-(C_{p_u} - C_{p_s})$ (where u denotes the measurement made during the interaction, and s is the time averaged measurement) is plotted on the vertical axis, with the chordal position of the transducers (x/c) on one axis, and the non-dimensional time (tV/c) on the axis in the foreground. For increased clarity, only every fifth result is presented.

On the upper surface (figure 3), where the axial flow is away from the blade surface, a strong suction peak is evident on the leading edge, where the vortex first encounters the blade. As it passes over the surface, this suction peak diminishes, but is still of significance over the entire chord of the blade.

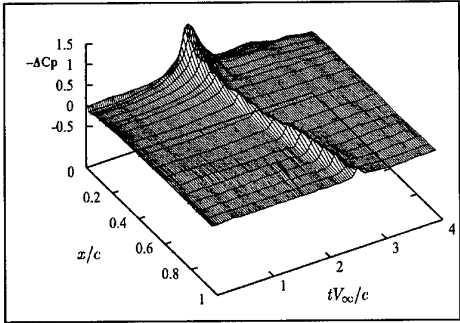


Figure3: Upper Surface Pressure Distribution

For the lower surface (figure 4), an increase in pressure is observed just downstream of the leading edge, but diminishes rapidly with the progression of the vortex over the chord of the blade. At approximately the quarter chord position, the suction ridge transforms into a slight suction ridge that continues to convect towards the trailing edge.

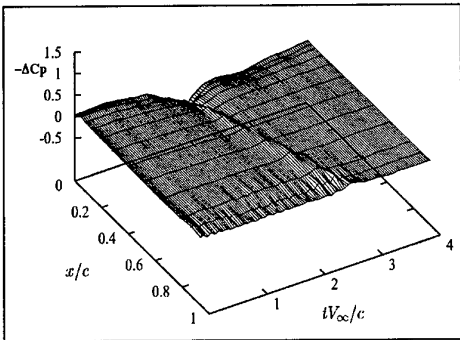


Figure 4: Lower Surface Pressure Distribution

These results clearly represent the complexity of the orthogonal interaction, and although only data for the centre of the vortex core is presented here, similar variations in the upper and lower surfaces may be observed for measurements above and below the core.

For this interaction, it is likely that a reduction in the axial core flow will occur once the vortex has been cut, significant enough to allow the low pressure in the vortex core to dominate, and hence producing the observed suction ridge over the surface. Entrainment of the boundary layer fluid on both sides of the blade after the initial severing has already been observed in water flow visualisation⁷, even in cases where a strong axial flow is present, which agrees with this assumption.

3.1.2 Normal Force and Pitching Moment

Through integration of the acquired pressure data over the surface of the blade, normal force (C_N) and quarter chord pitching moment (C_M) coefficients can be obtained. As the vortex is cut by the blade leading edge, a significant impulsive force is experienced by the blade, which decays as the vortex passes down the blade surface.

As the vortex approaches the blade, a large nose-up pitching moment is experienced by the blade. A rapid change of sign of this moment is subsequently observed, which may be attributed to the vortex passing over the quarter chord position. After the vortex passes over the trailing edge, the pre-interaction pitching moment values are recovered.

3.1.3 Pressure response to Incidence

The pressure response when the blade incidence is varied is of a very similar form to that observed for the zero incidence case. When the blade is set to negative incidence, although the form of the response is consistent, the pressure pulse on the lower surface is observed to increase in magnitude. Although the lower surface pressure distribution is altered for the blade set to incidence, the overall effect of the interaction on the transient normal force is the same as for the clean interaction case.

3.1.4 Secondary Interaction Characteristics

During the forward flight regime, it is reasonable to assume that the main rotor tip vortex may be cut several times by the tail rotor blades after the initial interaction has occurred. While considering the surface pressure data from the interaction of a pre-cut vortex with a blade in the orthogonal sense, it is possible to observe that the results are of a similar nature to the clean interaction, but of a reduced magnitude. The similarity would indicate that a complete vortex is in existence prior to the second interaction, and the extent of the similarity indicates that both rotational and axial components have been re-established within the vortex core.

This indicates that although a loss of momentum is experienced within the core, that complete destruction of the core does not occur. The main point of note for this interaction is the reduction in severity.

3.2 PIV measurement

3.2.1 Isolated vortex

To obtain data for the vortex prior to the interaction, the vortex was illuminated within the tunnel without the interacting blade present. By removing the mean u component from the velocity flow field, the vortex becomes clearly visible (figures 5a and b).

Measurements have shown that the vortex is approximately 15mm in diameter in the freestream, with a mean circulation strength of $0.58\text{m}^2\text{s}^{-1}$. By comparison of the severed vortex with the pre interaction case, attributes associated with the interaction may be clearly identified.

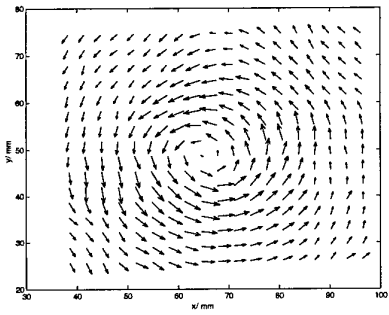


Figure 5a: Free vortex, mean u component removed (axis origin is arbitrary) maximum velocity 9.27 ms^{-1}

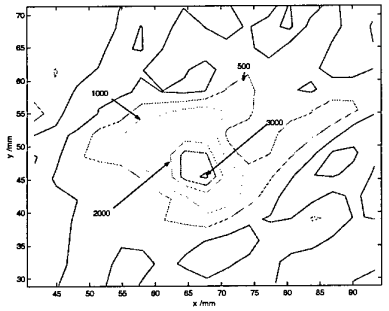


Figure 5b: Vorticity contours of free vortex (axis origin is arbitrary, contours values in s^{-1})

3.2.2 Orthogonal Interaction – Zero Degrees Incidence

By implementing the twin PIV system to capture the vortex as it passes over the leading edge position, it is possible to look at the immediate effect on the vortex core as it is severed by the blade. In order to track the progression of a single vortex over both sides

of the blade, images were obtained for the same vortex on either side of the blade at various positions along the blade surface. Results obtained like this have allowed verification of data obtained for separate runs on the blade surface, as well as providing a direct comparison.

The lightsheets were positioned at 15mm from the blade centre line, as previous measurements of the interaction have shown no significant change in the structure of the vortex core at a distance of 30mm from the blade chord line. The distance of 15mm was chosen as the closest position to the blade surface (at the maximum thickness the sheet was at 3.5mm from the blade surface) without leading to the production of adverse background illumination. The presented images give the x-axis relative to the blade leading edge at zero. The divergence and vorticity contour plots all present the contour levels in s^{-1} .

Just prior to the interaction, there is no significant difference within the vortex core when compared to the undisturbed case (refer figure 5 (a) and (b)).

As the vortex passes over the leading edge position, and is severed, the axial flow is blocked by the blade on the lower surface. As this occurs, a spiralling motion outward of the vortex core becomes evident (figure 6a). This spiralling motion may be attributed to the presence of a radial outflow from the core, (figure 6b). It is the superposition of this radially outward flow onto the vortex flow which leads to the observed spiralling motion.

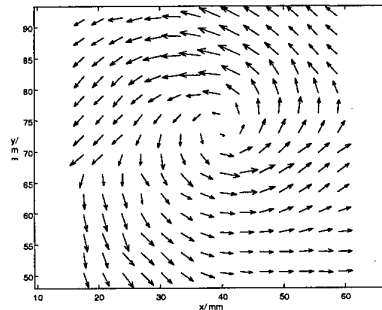


Figure 6a: Lower Surface velocity with mean u component removed. Maximum Velocity 9.39 ms^{-1}

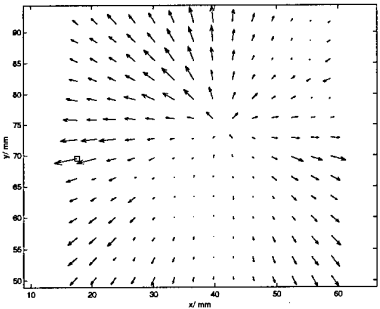


Figure 6b: Radial Outflow on the lower surface. Mean radial velocity 1.19ms^{-1}

As the vortex passes down the chord on the lower blade surface, the maximum vorticity levels decrease, although the vortex still maintains a coherent structure (compare figure 7 with the isolated vortex in figure 5b). This decrease in vorticity would be consistent with predictions that the vorticity within the core is redistributed radially outwards during the interaction.

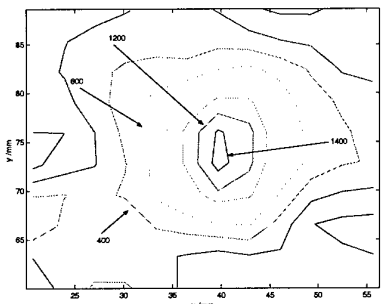


Figure 7 Lower surface vorticity

Associated with the lower surface interaction is the expected deceleration of the axial flow towards the blade surface as shown by the divergence (figure 8). As the progression of the vortex over the blade is tracked, it is observed that as a result of the interaction, the core continues to expand.

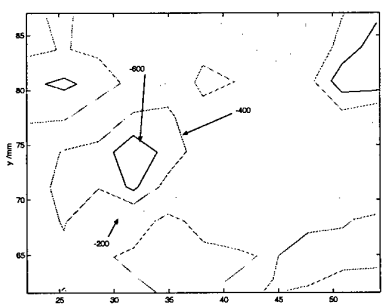


Figure 8 Divergence Contours over Lower Surface

On the upper blade surface, distortion within the vortex core is not as apparent as the radial outflow observed on the lower surface (figure 9a). By calculating the radial velocity components, a weak radial inflow can be seen (figure 9b), which would lead to a slight inward spiral motion. This radial inflow is persistent over the span of the blade.

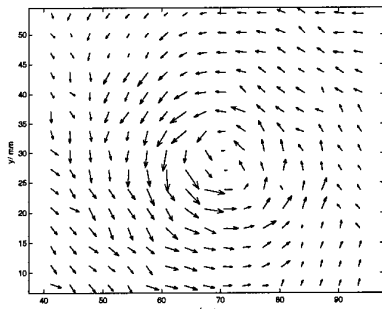


Figure 9a: Vortex velocity map. Maximum Velocity 8.35ms^{-1}

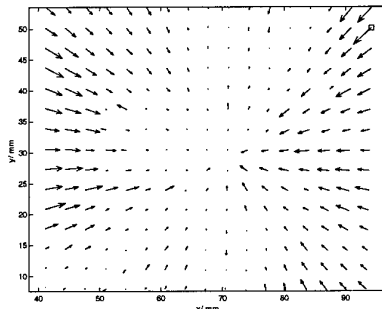


Figure 9b: Radial Inflow. Mean radial velocity -0.99ms^{-1}

Unlike the lower surface, the vorticity does not appear to be re-distributed, and a steady peak vorticity is maintained over the entire chord of the blade (figure 10).

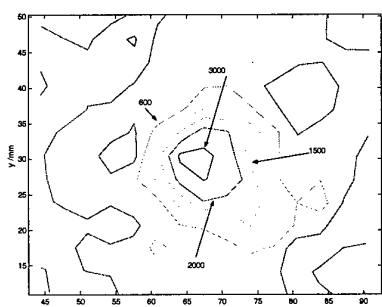


Figure 10: Vorticity Contours

The upper surface divergence patterns prove to be more complicated than those observed on the lower surface. The core region appears to be surrounded by areas of positive and

negative divergence (figure 11), almost in the form of a split, which persists over the surface of the blade. The divergence pattern obtained has been examined for possible errors due to spurious vectors by increasing the tile size, post-processing steps, and the use of a tile overlap. Even with the use of these methods, this pattern is still consistently apparent. The core on this side of the blade will require further examination, possibly through the use of a stereoscopic system.

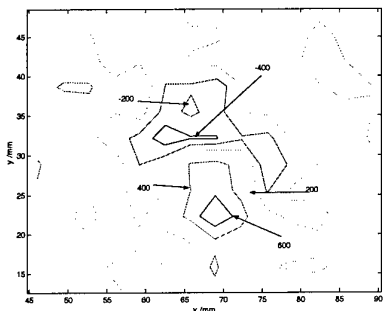


Figure 11: Divergence Pattern

Measurements tracking the variation in the vortex core were made on either side of the blade at the maximum thickness. Bulging of the core on the lower surface, and the associated thinning on the upper surface have both been of note in many previous studies. By moving the lightsheet away from the surface in 2mm increments, the flow was interrogated on both blade surfaces.

The bulging of the vortex core was apparent on the lower surface, with the core approximately 22mm in diameter at 15mm from the blade chord line, and quickly regaining its undisturbed state with increasing distance from the blade surface. As noted in previous studies, there was no evidence of the radial outflow at a distance of 27mm from the blade centreline, as the effect of the radial flow decreased rapidly through the core.

Variation in the core area was less evident on the upper surface, as it appeared to remain at approximately the undisturbed state, even close to the blade surface. The most striking difference through the core on the upper surface was the steep decrease in the radial component inducing the inward spiral, which decreased quickly with progression through the vortex core. As would be expected on both sides of the blade, the axial acceleration decreased quickly as the distance from the blade surface increased.

3.2.2 Trailing Edge Location

In order to interrogate the trailing edge location, the lightsheet was placed coincident with the chord line of the blade behind the trailing edge. The blade was then moved laterally so that comparative data could be obtained for the upper and lower surface locations.

When the core passes into the trailing edge region, a significant decrease in the maximum vorticity compared to the pre-interaction peak is observed (figure 12).

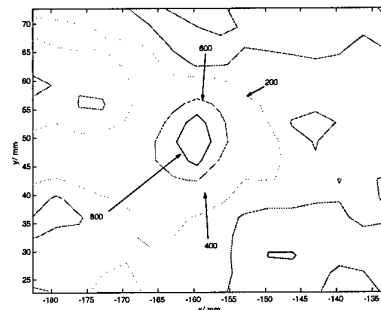


Figure 12: Trailing Edge Vorticity contours showing reduction in peak vorticity (compare with figure 5b)

There is no apparent radial flow within the vortex core, and although no evidence exists of whether a severed core is in existence, or if a rejoicing of the vortex core has occurred, there appears to be minimal, if any divergence in the axial flow direction, which would be consistent with the axial flow being regenerated through the core and passing through at a constant velocity. The wake of the interacting blade appears to lead to little or no distortion of the vortex core in this region.

3.3.3 Effect of Blade Incidence

The incidence of the interacting blade relative to the mean flow direction was increased in the negative sense, and the flow about the leading edge region was interrogated for the lower surface interaction.

As the blade incidence is increased, the local flow velocity over the leading edge region of the blade increased, as would be expected (figure 13).

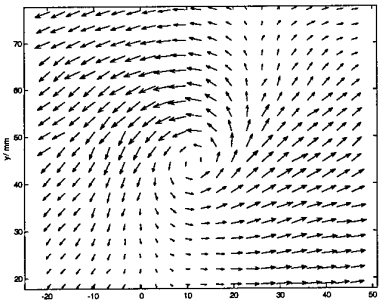
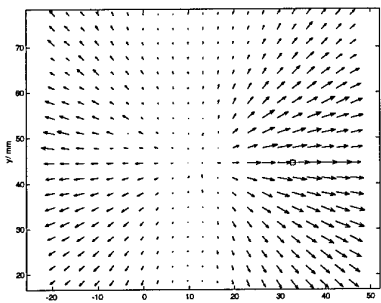


Figure 13: Mean flow velocity over the leading edge (-8°). Maximum velocity 9.0ms⁻¹

Associated with this is an increase in the maximum velocity of the radial outflow from the vortex core (figure 14).



**Figure 14 : Radial Outflow (-8° incidence)
Mean radial velocity 2.82ms⁻¹**

The peak vorticity levels within the vortex do not appear to diminish in the same manner as is observed for the zero degrees incidence case, remaining comparable to those of the freestream vortex (figure 15). This would indicate that the effect of the radial component on the vortex is decreasing with increasing incidence.

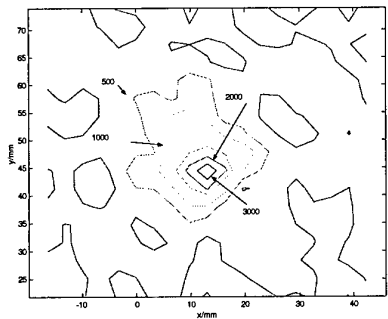


Figure 15: Vorticity contours (-8° incidence)

The divergence contours show no variation in overall pattern to those obtained for the zero degrees incidence, so it can be assumed that

the changing incidence has no real effect on the axial flow behaviour in the leading edge region.

4 Discussion

Over the lower and upper surfaces, the radial flow that is promoted within the vortex core due to the severing of the vortex core has been identified – a radial outflow on the lower surface, and a corresponding, weaker radial inflow on the upper surface. In order to further quantify the effect of this radial flow on the vortex, a simple potential flow model may be employed, which considers the flow as a point source or sink superimposed on a vortex.

The source models the radial flow observed in the experiments. If the flow field of a potential vortex superimposed on a potential source is considered, it may be easily shown that there is a line of zero u component at an angle $\tan\theta_u = -q / \Gamma$ to the x-axis and a line of zero v component at an angle $\tan\theta_v = \Gamma / q$ to the x-axis. If we isolate the u and v components of the BVI flow fields obtained using PIV, patterns consistent with the above model are observed. Figures 16a and 16b show the isolated u and v components from figure 6a, the interaction on the lower surface. The zero u component line runs from the bottom right towards the top left of the image, while the zero v component line runs from the bottom left to the top right of the image. From these images the ratio of source strength to vortex strength is approximately 0.48. The divergence patterns indicate that the radially outward mass flow is derived from a large area; the current simple model helps quantify the overall mass flow effect.

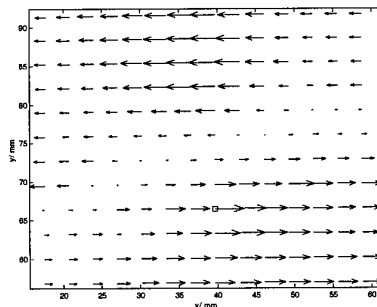


Figure 16a: Isolated u components

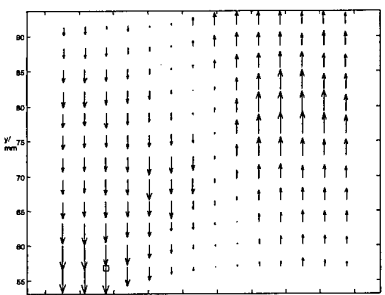


Figure 16b: Isolated v components

The upper surface interaction has already been observed to be much weaker than the lower surface interaction, and it is too weak to be clear on the isolated u and v component plots (not shown). This simply indicates that the sink strength is very low. However, the divergence pattern over the upper surface is more complex than that over the lower surface. It is conceptually clear that the upper surface interaction is more complex than that over the lower surface. The axial flow within the vortex is directed towards the lower surface and away from the upper surface. Therefore the vortex axial flow component must simply reduce towards the lower surface, while for the upper surface the axial flow component must be re-established further away from the blade. Negative divergence indicates a transfer of mass flow from the vortex axial direction into the x-y plane. The small zone of low negative divergence could be indicating the necessary deceleration of the axial flow very close to the surface (the laser sheet is only 3.5mm away from the blade surface at $x=40\text{mm}$). On the other hand the positive divergence might be indicating a mass transfer from the x-y plane to the direction away from the blade surface for the re-establishment of the vortex axial flow further from the blade surface. This is a tentative suggestion, and clearly more experimentation is necessary for the flow over the upper surface.

By considering the variation in the ratio of the source to vortex with the increasing incidence, the effect of the radial component on the vortex does appear to decrease, as is indicated by the vorticity contours (see figure 15). Figure 14 suggests a higher source strength for the zero incidence case. However, the pressure data indicates a stronger interaction, which suggests less expansion of the vortex core. The reduction in the ratio of source to vortex strength resolves the ambiguity arising from figure 14.

5 Further Work

The effects on the core will require to be further investigated in the boundary layer region to assess the effect of the interaction at this level, and the effect of the boundary layer fluid on the vortex interaction on either side of the interacting blade.

It is also anticipated that a further study of the trailing edge location will be carried out in order to fully establish the behaviour of the two halves of the core after they pass into the trailing edge region and whether rejoining of the vortex core occurs. The effect of the blade incidence would also be considered for this.

The need for further investigation of the upper surface axial flow has already been commented upon, and it is expected that a stereoscopic interrogation of this region will be possible. The stereoscopic system would also allow for further study of the interaction at all points on the surface of the blade.

6 Conclusions

The orthogonal blade-vortex interaction has been investigated using unsteady pressure measurements and particle image velocimetry.

As the vortex core is severed by the interacting blade, a pressure pulse was formed on the lower surface and a strong suction peak on the upper surface.

On the lower surface, where the vortex axial flow was directed towards the blade surface, a distortion in the vortex core due to the impingement of the axial flow on the surface occurred. This was of the form of a radial outflow, which led to a re-distribution of vorticity in the core, and a decrease in the peak vorticity levels as the core progressed down the chord line. On the upper surface, where the axial flow is away from the blade, a radial inflow was observed post interaction, but appeared to preserve the vorticity level within the core.

Calculation of the divergence for the interaction allowed an analysis of the mass flow within the vortex core, and the variations within the vortex core axial flow during the interaction.

It was shown that a simple model of the interaction is obtained by consideration of the behaviour of potential sources and vortices.

By increasing the incidence of the blade in the negative sense, the pressure pulse on the lower surface could be seen to increase in magnitude, while the effect of the radial outflow on the vortex decreased.

In the trailing edge region, there is evidence that rejoining of the two halves of the vortex core may occur, with the re-establishment of radial and axial flow components in a weakened state.

On either side, there was no significant disturbance to the vortex core as the laser sheet was moved further away from the blade surface.

Acknowledgements

This material is based upon work supported by the European Research Office of the US Army under Contract No.N68171-00-M-5988. Any opinions, findings and conclusions or recommendations expressed in this material are those of the authors, and do not necessarily reflect the views of the European Research Office of the US Army.

Work undertaken into the acquisition of surface pressure data was funded by the Engineering and Physical Research Council (EPSRC), the British Ministry of Defence (MOD), the Defence Evaluation and Research Agency, Farnborough and GKN-Westland Helicopters Ltd under grant number GR/L 58231 through the EPSRC/MOD joint grants scheme.

References

- 1 Green RB; Doolan CJ (1999)** PIV measurements of the orthogonal blade-vortex interaction. 3rd International Workshop on PIV: paper 136, Santa Barbara
- 2 Howe, MS (1989)** On the unsteady surface forces, and sound produced by the normal chopping of a rectilinear vortex. J. Fluid Mechanics 206, p 131-153
- 3 Krishnamoorthy S; Marshall JS (1994)** An experimental investigation of 'vortex shocks'. Phys. Fluids A, vol 6, no 11
- 4 Marshall JS; Yalamanchili R (1994)** Vortex cutting by a blade, Part II:
- Computations of Vortex Response. AIAA J., Vol 32, no 7: 1428-1436
- 5 Marshall JS; Grant JR (1996)** Penetration of a blade into a vortex core : vorticity response and unsteady blade forces. J. Fluid Mech, vol 306: 83-109
- 6 Marshall JS (1994)** Vortex cutting by a blade, Part I: general theory and a simple solution. AIAA J., vol 32, no 6 :1145-1150
- 7 Marshall JS; Krishnamoorthy S (1997)** On the instantaneous cutting of a columnar vortex with non-zero axial flow. J. Fluid Mech 351: 41-74
- 8 Lee JA; Burggraf OR; Conlisk AT (1997)** On the impulsive blocking of a vortex jet. J. Fluid Mech 369 : 301-331
- 9 Green RB; Doolan CJ; Cannon RM (2000)** Measurements of the orthogonal blade-vortex interaction using a particle image velocimetry technique. Exp. Fluids 29 : 369-379
- 10 Copland CM (1997)** The generation of transverse and longitudinal vortices in low-speed wind tunnels. Ph.D. Thesis, Department of Aerospace Engineering, University of Glasgow, Scotland, UK
- 11 Doolan CJ, Green RB; Coton FN; Galbraith RAMcD (2000)** The Orthogonal Blade-Vortex Interaction Experimental Programme at the University of Glasgow. European Rotorcraft Forum.
- 12 Copland CM; Coton FN; Galbraith RAMcD (1998)** A study of Helicopter Tail Rotor Interaction: Phase 1 – Proof of Concept. 24th European Rotorcraft Forum, Marseilles, France
- 13 Raffel M, Willert C; Kompenhaus J (1998)** Particle Image Velocimetry. Springer-Verlag
- 14 Adrian, RJ (1991)** Particle-Imaging Techniques for Experimental Fluid Mechanics. Annu. Rev. Fluid Mech 23 : 261-304
- 15 Noguiera J; Lecouna A; Rodriguez PA (1997)** Data validation, false vector correction and derived magnitudes calculation on PIV data. Meas Sci Tech 8 :1493-1501

